ELSEVIER

Journal of Alloys and Compounds 404–406 (2005) 55–59

Journal of ALLOYS AND COMPOUNDS

www.elsevier.com/locate/jallcom

Atom relaxations around hydrogen defects in lanthanum hydride

G. Renaudin[a], K. Yvon[a], W. Wolf[b], P. Herzig[c,*]

[a] *Laboratoire de Cristallographie, Université de Genève, CH-1211 Genève, Switzerland*
[b] *Materials Design s.a.r.l., 44, av. F.-A. Bartholdi, 72000 Le Mans, France*
[c] *Institut für Physikalische Chemie, Universität Wien, Währinger Straße 42, 1090 Vienna, Austria*

Received 29 July 2004; received in revised form 14 February 2005; accepted 18 February 2005
Available online 14 July 2005

Abstract

Atom relaxations around empty octahedral and tetrahedral metal interstices in cubic lanthanum hydride LaH_{2+x} have been studied experimentally and by ab initio theory. In-situ neutron powder diffraction data on the deuteride along the pressure–composition isotherm at 573 K reveal deuterium atom displacements of up to 0.6 Å within octahedral interstices. The displacements are directed from the centres towards the faces of the metal octahedra and are largest at deuterium contents of $x \sim 0$, i.e. in the presence of nearly empty octahedral and nearly filled tetrahedral interstices. As the deuterium content is increased the displacements decrease sharply and then increase slowly. Ab initio calculations on nearly stoichiometric LaH_3 ($La_{32}H_{95}$) confirm energetically favoured atom relaxations around empty hydrogen sites. The relaxations around tetrahedral vacancies are considerably larger than those around octahedral vacancies. Deuterium atoms in octahedral interstices, for example, relax by up to 0.8 Å which compares well with experiment. Empty metal tetrahedra contract by 0.06 Å while empty octahedra expand by 0.02 Å. Due to the strong relaxations around tetrahedral vacancies, formation of tetrahedral vacancies in LaH_3 is less favourable by just about 4 kJ mol^{-1} than formation of octahedral vacancies.

Keywords: Rare-earth hydrides; Gas–solid reactions; Crystal structure; Hydrogen defects; Ab initio calculations; In-situ neutron diffraction

1. Introduction

Rare-earth (R)–hydrogen systems display a variety of interesting phenomena [1,2] among which hydrogen induced metal–insulator transitions are a favoured subject of current research [3,4]. All systems contain a cubic hydride phase of composition RH_{2+x} whose upper phase limit decreases from $x = 1$ (La) to $x \sim 0$ (Lu) as one proceeds from light to heavy R elements. The hydrogen atoms in this phase occupy tetrahedral and octahedral interstices of a cubic-close-packed (ccp) metal atom arrangement. Those in the octahedral interstices are not located at the centre but are more-or-less displaced towards the octahedron faces. In a recent study it was pointed out [5] that these displacements decrease as a function of atomic size of R. In view of their possible role in the metal–insulator transition and their possible influence on the upper phase limit of the cubic RH_{2+x} phase it was decided to investigate the displacements in a particular system as a function of hydrogen content and to compare them with quantum-theoretical calculations. For this purpose a deuterated lanthanum sample was examined by in-situ neutron powder diffraction as a function of deuterium pressure, and ab initio calculations were performed. Phase diagram data [6,7] suggested that temperatures close to 550 K and pressures between $\sim 10^{-2}$ mbar and 10 bar provide a favourable pressure–composition regime for such a study.

2. Experimental

2.1. Sample preparation

A powder sample was prepared by deuteration of lanthanum metal (pieces, 99.99% purity) in an autoclave. In a

* Corresponding author. Fax: +43 1 4277 9524.
E-mail address: peter.herzig@univie.ac.at (P. Herzig).

0925-8388/$ – see front matter © 2005 Elsevier B.V. All rights reserved.
doi:10.1016/j.jallcom.2005.02.079

first step the temperature was increased to 673 K during 1 day under a deuterium gas pressure of about 100 bar. In a second step the deuterium pressure was released by evacuating the autoclave to 10^{-2} mbar and the temperature was increased to 773 K during 1 day. The autoclave was air-quenched and opened in an argon-filled glove box. The resulting sample was single-phase and consisted of cubic LaD_{2+x}.

2.2. Neutron powder diffraction

The deuterium atom distribution was investigated by in-situ neutron powder diffraction on the HRPT instrument [8] at SINQ (PSI, Villigen, Switzerland). A sample of ∼ 6 g mass was enclosed in cylindrical steel containers of 8 mm inner diameter and connected to a vacuum pump and deuterium pressure control system. The deuterium pressure was applied by a portable automatic flow/pressure computer controller adapted for pcT-isotherm measurements built at the Physics Department of the University of Fribourg (Switzerland). This system was equipped with a heating furnace (maximum deuterium pressure ∼ 10 bar at maximum temperature of ∼ 600 K). In order to characterise the samples at their lowest deuterium contents as recommended by Vajda [2], data were first recorded by evacuating the sample (∼ 10^{-2} mbar) for one night at 573 K. In the following, the deuterium pressure was increased at constant temperature (573 K) and data were recorded at 18 deuterium pressures ranging from 2 mbar to 7.1 bar (see Table 1). The experimental conditions were $\lambda = 1.1965$ Å, 2θ range 3–163°, step size $2\theta = 0.05°$, 4 h counting time at each pressure, summing 12 patterns of 20 min each in the same temperature and pressure conditions. Between two consecutive measurements the sample was kept ∼ 30 min at the new pressure in order to reach equilibrium. Non-equilibrium data were identified by monitoring each run and removed from structural refinement whenever possible. The patterns contained no impurity peaks except for those due to the steel container.

2.3. Structure refinement

Rietveld refinements (program *FullProf.2000* [9]) were performed based on the known structural parameters of cubic LaD_{2+x} (space group $Fm\bar{3}m$, La on site 4*a* (0,0,0, etc.), deuterium in tetrahedral interstices, D_{tetra}, on site 8*c* (1/4,1/4,1/4, etc.) and octahedral interstices, D_{octa}, on site 4*b* (1/2,1/2,1/2, etc.)). In a first step, D_{octa} was left at the centre of the octahedral interstices (position 4*b*), and in a second step it was allowed to move along ⟨1 1 1⟩ to off-centre positions having lower symmetry (site 32*f* *x*, *x*, *x*, etc.). All data sets lead to positional parameters for D_{octa} that differed significantly from $x = 1/2$. Similar displacements for D_{tetra} were not found to occur to a significant extent, and thus, were not taken into account during structure refinement. In order to increase the stability of the refinements the temperature factor of D_{octa} was constrained to be the same as that of D_{tetra}. Up to 28 parameters were refined: 12 profile parameters (Thompson-Cox-Hastings pseudo-Voigt peak-shape function with an asymmetry correction), six coefficients for the background polynomial function, one zero shift plus sample displacement and transparency, one scale factor, one cell parameter, two deuterium site occupancy factors, two isotropic temperature factors (one for the R site and one for the two deuterium sites) and one positional parameter for D_{octa}. For patterns recorded under deuterium pressures of 10 mbar and above, the occupancy of D_{tetra} did not significantly deviate from unity, and thus, was fixed at unity. Refinement results are summarised in Table 1 and interatomic distances are given in Table 2. The off-centre displacements, ε, of D_{octa} as a function of refined deuterium content are shown in Fig. 1.

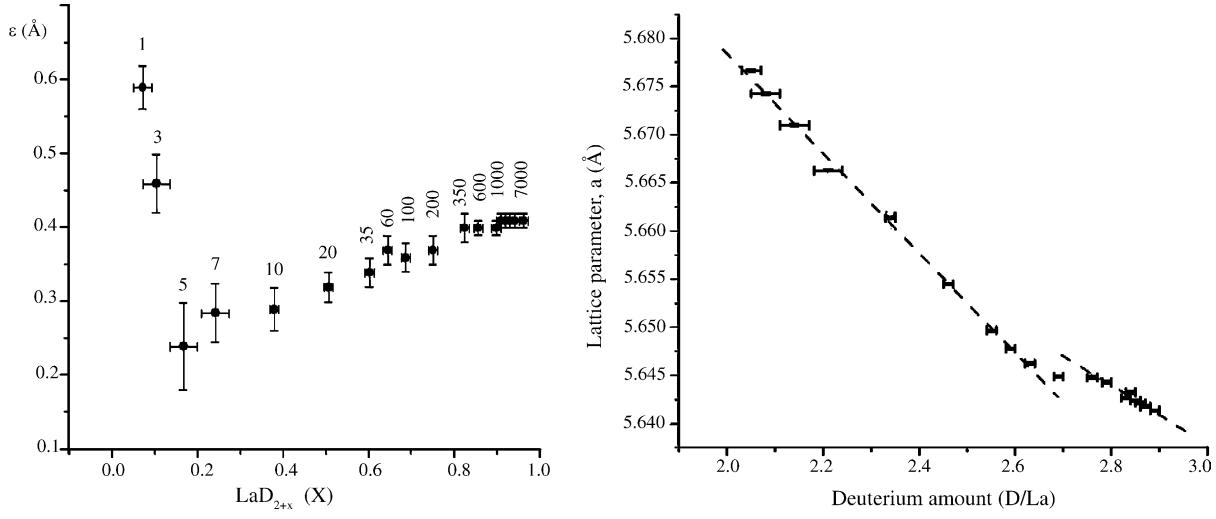

Fig. 1. Left: refined average deuterium atom displacements (ε) in octahedral interstices as a function of refined composition for LaD_{2+x}. The applied in-situ deuterium pressure during the neutron diffraction experiment is indicated in mbar. Error bars correspond to one e.s.d. ($\pm\sigma$). Right: lattice parameter *a* for LaD_{2+x} as a function of composition.

Table 1
Refinement results for cubic LaD_{2+x} on neutron powder diffraction data at 573 K and different deuterium pressures (e.s.d.'s in parentheses)

D_2 pressure	Refined composition	Cell parameter a (Å)	$x(D_{octa})$ site $32f$ x, x, x	Occupancy of interstices*		Temperature factor B (Å^2)**		Rietveld agreement indices		
				D_{octa}	D_{tetra}	La	D	R_p	R_{wp}	χ^2
2 mbar	$LaD_{2.05(3)}$	5.6767(1)	0.440(3)	0.13(1)	0.96(1)	1.61(3)	2.57(4)	9.3	8.2	9.4
3 mbar	$LaD_{2.08(3)}$	5.6743(1)	0.453(4)	0.15(1)	0.96(1)	1.61(4)	2.60(5)	9.5	8.5	6.1
5 mbar	$LaD_{2.14(3)}$	5.6710(1)	0.476(6)	0.19(1)	0.97(1)	1.48(5)	2.8(1)	9.5	8.4	6.1
7 mbar	$LaD_{2.21(3)}$	5.6663(1)	0.471(4)	0.26(1)	0.98(1)	1.51(5)	2.82(9)	9.6	8.4	6.1
10 mbar	$LaD_{2.34(1)}$	5.6614(1)	0.470(3)	0.34(1)	1(−)	1.59(5)	2.8(1)	9.7	8.4	6.2
20 mbar	$LaD_{2.46(1)}$	5.6545(1)	0.467(2)	0.46(1)	1(−)	1.61(5)	2.87(9)	9.6	8.3	6.1
35 mbar	$LaD_{2.55(1)}$	5.6497(1)	0.465(2)	0.55(1)	1(−)	1.66(5)	2.84(9)	9.6	8.3	6.1
60 mbar	$LaD_{2.59(1)}$	5.6478(1)	0.462(2)	0.59(1)	1(−)	1.73(5)	2.73(8)	10.0	8.6	6.5
0.1 bar	$LaD_{2.63(1)}$	5.6463(1)	0.463(2)	0.63(1)	1(−)	1.75(5)	2.74(9)	9.9	8.6	6.5
0.2 bar	$LaD_{2.69(1)}$	5.6449(1)	0.462(2)	0.69(1)	1(−)	1.79(5)	2.68(8)	10.0	8.6	6.4
0.35 bar	$LaD_{2.76(1)}$	5.6448(1)	0.459(2)	0.76(1)	1(−)	1.75(6)	2.59(9)	11.6	9.9	4
0.6 bar	$LaD_{2.79(1)}$	5.6443(1)	0.459(1)	0.79(1)	1(−)	1.75(6)	2.59(8)	10.8	9.3	7.1
1 bar	$LaD_{2.84(1)}$	5.6433(1)	0.458(1)	0.84(1)	1(−)	1.80(6)	2.53(8)	11.8	10.1	4.1
1.5 bar	$LaD_{2.83(1)}$	5.6427(1)	0.459(1)	0.83(1)	1(−)	1.84(5)	2.57(7)	10.0	8.7	6.7
2 bar	$LaD_{2.85(1)}$	5.6424(1)	0.458(1)	0.85(1)	1(−)	1.87(5)	2.54(6)	10.0	8.6	6.6
3 bar	$LaD_{2.86(1)}$	5.6422(1)	0.458(1)	0.86(1)	1(−)	1.87(5)	2.52(6)	10.0	8.6	6.6
5 bar	$LaD_{2.87(1)}$	5.6418(1)	0.458(1)	0.87(1)	1(−)	1.88(5)	2.55(7)	10.1	8.7	6.8
7.1 bar	$LaD_{2.89(1)}$	5.6414(1)	0.458(1)	0.89(1)	1(−)	1.89(5)	2.53(6)	10.0	8.7	6.7

* Population parameter of D_{octa} on site $32f$ multiplied by 8.
** Form of temperature factor: $T = \exp[-B_{iso}(\sin\theta/\lambda)^2]$.

3. Ab initio calculations

Vacancy formation energies and atom displacements around vacancy sites have been studied by ab initio calculations with the Vienna Ab-initio Simulation Package (VASP) [10,11]. The calculations are based on density functional theory [12,13] within the generalized gradient approximation [14] for many-body effects such as exchange and correlation. A plane wave basis set with a cutoff energy of 250 eV was applied and the projector augmented wave technique [15,16] was used to accurately describe the electron-ion interactions. Vacancies were described within a $2 \times 2 \times 2$ supercell model of the conventional unit cell of LaH_3 with an overall stoichiometry of $La_{32}H_{95}$. For these supercells, a $3 \times 3 \times 3$ Monkhorst Pack mesh [17] and Methfessel Paxton integration [18] with a broadening parameter of 0.2 eV was used for sampling the Brillouin zone. Displacements of atoms in the vicinity of octahedral and tetrahedral vacancies were calculated by minimizing atomic forces of all atoms within supercells of $R\bar{3}$ and $R3$ symmetry, respectively. The calculated lattice parameter of 5.57 Å for LaH_3 is in good agreement with experimental data, and was not further modified for off-stoichiometric supercells. The calculated relaxations around tetrahedral and octahedral hydrogen vacancy sites are summarized in Fig. 2.

Table 2
La—D bond distances, D–D contact distances and D_{octa} displacements ε (Å) for cubic LaD_{2+x} at 573 K and various deuterium pressures (e.s.d.'s in parentheses)

D_2 pressure	La–D_{tetra}	La–D_{octa}	La–$D_{octa(c)}$*	D_{tetra}–D_{octa}	D_{tetra}–$D_{octa(c)}$*	ε: D_{octa}–$D_{octa(c)}$*
2 mbar	2.4581(1)	2.54(3)	2.8384(1)	1.87(3)	2.4581(1)	0.59(3)
3 mbar	2.4571(1)	2.60(4)	2.8372(1)	2.00(4)	2.4571(1)	0.46(4)
5 mbar	2.4557(1)	2.70(6)	2.8356(1)	2.22(6)	2.4557(1)	0.24(6)
7 mbar	2.4536(1)	2.68(4)	2.8332(1)	2.16(4)	2.4536(1)	0.28(4)
10 mbar	2.4515(1)	2.67(3)	2.8307(1)	2.15(3)	2.4515(1)	0.29(3)
20 mbar	2.4485(1)	2.65(2)	2.8273(1)	2.13(2)	2.4485(1)	0.32(2)
35 mbar	2.4464(1)	2.64(2)	2.8249(1)	2.10(2)	2.4464(1)	0.34(2)
60 mbar	2.4456(1)	2.63(2)	2.8239(1)	2.07(2)	2.4456(1)	0.37(2)
0.1 bar	2.4450(1)	2.63(2)	2.8232(1)	2.08(2)	2.4450(1)	0.36(2)
0.2 bar	2.4444(1)	2.62(2)	2.8225(1)	2.07(2)	2.4444(1)	0.37(2)
0.35 bar	2.4443(1)	2.61(2)	2.8225(1)	2.04(2)	2.4443(1)	0.40(2)
0.6 bar	2.4441(1)	2.61(1)	2.8222(1)	2.04(1)	2.4441(1)	0.40(1)
1 bar	2.4437(1)	2.61(1)	2.8217(1)	2.03(1)	2.4437(1)	0.41(1)
1.5 bar	2.4434(1)	2.61(1)	2.8214(1)	2.04(1)	2.4434(1)	0.4(1)
2 bar	2.4433(1)	2.61(1)	2.8212(1)	2.03(1)	2.4433(1)	0.41(1)
3 bar	2.4432(1)	2.61(1)	2.8211(1)	2.03(1)	2.4432(1)	0.41(1)
5 bar	2.4430(1)	2.61(1)	2.8209(1)	2.03(1)	2.4430(1)	0.41(1)
7.1 bar	2.4428(1)	2.61(1)	2.8207(1)	2.03(1)	2.4428(1)	0.41(1)

* $D_{octa(c)}$: centre of La octahedron.

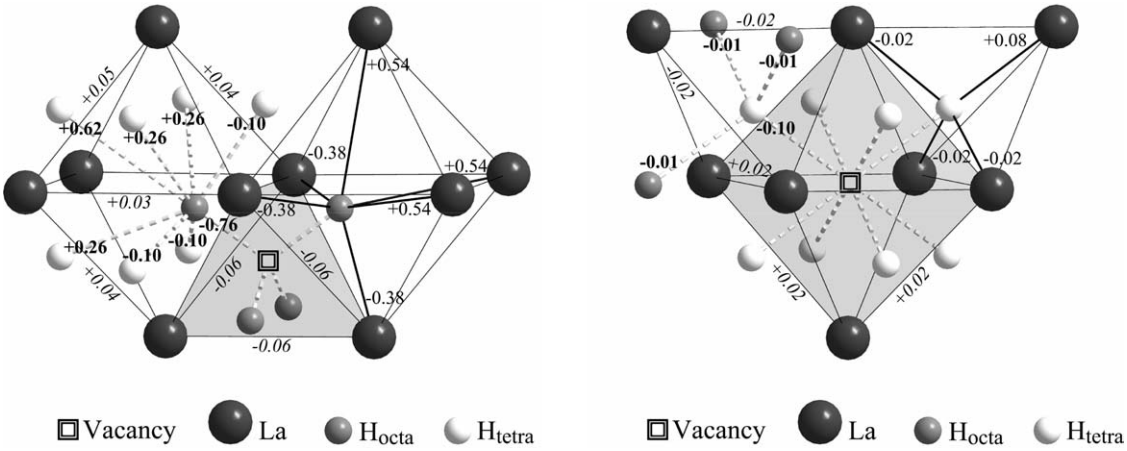

Fig. 2. Calculated atom relaxations (Å) around tetrahedral (left, point group $\bar{4}3m$) and octahedral (right, point group $m\bar{3}m$) hydrogen vacancy in $La_{32}H_{95}$. Bold: H–H and vacancy–H; normal: H–La; italic: La–La. Interatomic distances in unrelaxed cubic structure (space group $Fm\bar{3}m$): vacancy–H_{octa} = vacancy–La = H_{octa}–H_{tetra} = 2.41 Å, H_{octa}–La = 2.79 Å, La–La = 3.94 Å.

4. Results and discussion

The structural changes of LaD_{2+x} as a function of deuterium pressure at 573 K can be described as follows. As the deuterium pressure increases the occupancy of the nearly filled tetrahedral interstices increases from 96% at 2 mbar ($x = 0.05$) to 100% at 0.01 bar ($x = 0.34$) and above, while the occupancy of the nearly empty octahedral interstices increases from 13% at 2 mbar to 89% at 7.1 bar ($x = 0.89$) (see Table 1). The fact that the occupancy of octahedral interstices starts before the tetrahedral interstices are completely filled (2 mbar: 13% octahedral versus 96% tetrahedral occupancy) is consistent with early NMR work [19], and is in line with similar data obtained under the same conditions for the neodymium analogue $NdD_{1.81}$ (8% octahedral versus 86% tetrahedral occupancy, unpublished results). As for the average displacements of the D_{octa} atoms away from their centres they are largest at low deuterium contents ($\varepsilon = 0.59$ Å at $x = 0.05$) and decrease abruptly to a minimum ($\varepsilon = 0.24$ Å at $x = 0.14$) before increasing slowly at higher deuterium contents ($\varepsilon = 0.41$ Å at $x = 0.89$) (see Table 2 and Fig. 1). These displacements lead to a considerable shortening of the La–D bonds and to closer contacts between deuterium atoms in neighbouring octahedral and tetrahedral interstices (see Table 2). As expected, the shortest La–D bonds and D–D contacts are associated with the largest displacements (La–D_{octa} = 2.54 Å and D_{tetra}–D_{octa} = 1.87 Å at $x = 0.05$ and $\varepsilon = 0.59$, as compared to 2.84 and 2.46 Å, respectively, for D_{octa} on centre position) and the longest La–D bonds and D–D contacts with the smallest displacements (La–D_{octa} = 2.70 Å and D_{tetra}–D_{octa} = 2.22 Å at $x = 0.14$ and $\varepsilon = 0.24$, as compared to 2.84 and 2.46 Å, respectively, for D_{octa} on centre position). As for the La–D_{tetra} bonds they are systematically shorter than the La–D_{octa} bonds and decrease continuously as a function of D content (from 2.46 Å at $x = 0.05$ to 2.44 Å at $x = 0.89$). Finally, there occurs a break in the variation of the lattice parameter versus composition around the composition $LaD_{2.8}$ (Fig. 1, right) which can be attributed to the well-known metal to insulator transition [3,4]. However, the resolution of the present data does not allow one to correlate this feature with other structure parameters such as D atom occupancies and/or interatomic distances.

The ab-initio calculations represent stoichiometries LaH_{2+x} with $x = 1$ and 0.97, thus addressing the limit of almost completely filled interstices, or from an alternative viewpoint, the limit of rather dilute vacancy concentrations in LaH_3. From the calculated total energies of the model structures, the preference for formation of vacancies on tetrahedral versus octahedral hydrogen sites was evaluated. Without taking into account lattice relaxation in the vicinity of the defects, removal of octahedral hydrogen from the trihydride is much easier (34 kJ mol^{-1}) than removal of tetrahedral hydrogen (93 kJ mol^{-1}). However, relaxation around the tetrahedral vacancy site is rather drastic, saving about 66 kJ mol^{-1}, whereas the relaxation effect around octahedral vacancies is rather moderate, lowering the energy just by about 10 kJ mol^{-1}. Thus, lattice relaxation around the tetrahedral vacancy site compensates for much of the extra energy required for its formation. The net energy required for formation of a tetrahedral vacancy is 28 kJ mol^{-1}, being just 4 kJ mol^{-1} larger than the energy of about 24 kJ mol^{-1} required for generating octahedral vacancies in LaH_3. The energies are with respect to isolated hydrogen molecules calculated within the same ab-initio approach.

The rather different energies calculated for relaxations around tetrahedral and octahedral vacancy sites are also reflected by the resulting distortions around the defects, as shown in Fig. 2. The distortions around tetrahedral vacancies are considerably larger than those around octahedral vacancies. Hydrogen atoms in octahedral interstices adjacent to tetrahedral vacancies move by about 0.76 Å towards the vacancy, which compares well with the magnitude of distortions

observed experimentally. Hydrogen atoms in tetrahedral interstices adjacent to octahedral vacancies move by about 0.1 Å towards the vacancy. In this case, comparison to experimental data is not feasible because of lack of resolution of the measured data. In addition to the distortions for the hydrogen sublattice, sizeable distortions are also seen for the La sublattice: empty metal tetrahedra contract by 0.06 Å and empty metal octahedra expand by 0.02 Å. The expansion of empty octahedra is consistent with experimental findings in ordered tetragonal $NdD_{2.27}$ [20] but cannot be seen in the present experiment, since resolution of data does not allow one to relax the La atoms in structure refinements. For similar reasons, the contraction of the empty metal tetrahedra can also not be seen by the present experiment. It is emphasized here that only average relaxations can be measured by the applied experimental techniques.

As a final step of the calculations, the vacancy site of the relaxed supercells $La_{32}H_{95}$ were filled with hydrogen and all atom positions were again optimized. As a result, the lattice of the undistorted LaH_3 model structure was recovered. It can therefore be concluded that the distortions of the hydrogen sublattice observed experimentally are caused by vacancy defects.

5. Conclusion

The atom relaxations in the LaH_{2+x} structure system are of major interest for the study of metal–insulator transitions in this and related systems. Given that the transitions usually occur at slightly sub-stoichiometric compositions they are bound to be affected by such relaxations. The latter could also be related to the observed decrease in the homogeneity range of the cubic hydride phase of heavy rare-earth elements. More work is in progress.

Acknowledgements

This work was supported by the Swiss National Science Foundation and the Swiss Federal Office of Energy. Thanks are due to D. Sheptiakov (PSI, Villigen) for help with the neutron data collections and to A. Züttel (University of Fribourg) for use of the high-pressure system. Partial support by the Austrian Science Foundation (Project No. P15801-N02) is gratefully acknowledged. The ab initio calculations were performed on the Schrödinger II Linux cluster of the Vienna University Computer Centre.

References

[1] R.R. Arons, in: H.P.J. Wijn (Ed.), Landolt-Börnstein, New Series III, vol. 19d1, Springer–Verlag, Berlin, 1991, p. 280.
[2] P. Vajda, K.A. Gschneidner Jr., L. Eyring (Eds.), Handbook on the Physics and Chemistry of Rare Earths, vol. 20, North-Holland, 1995, p. 209.
[3] R. Griessen, J.N. Huiberts, M. Kremers, A.T.M. van Gogh, N.J. Koeman, J.P. Dekker, P.H.L. Notten, J. Alloys Compd. 253–254 (1997) 44.
[4] K.K. Ng, F.C. Zhang, V.I. Anisimov, T.M. Rice, Phys. Rev. Lett. 78 (1997) 1311.
[5] G. Renaudin, P. Fischer, K. Yvon, J. Alloys Compd. 330–332 (2002) 175.
[6] R.N.R. Mulford, C.E. Holley Jr., J. Phys. Chem. 59 (1955) 1222.
[7] C. Ohki, H. Uchida, C. Huang, Z. Phys. Chem. N. F. 163 (1989) 149.
[8] P. Fischer, G. Frey, M. Koch, M. Könnecke, V. Pomjakushin, J. Schefer, R. Thut, N. Schlumpf, R. Bürge, U. Greuter, S. Bondt, E. Berruyer, Physica B 276–278 (2000) 146.
[9] J. Rodriguez-Carvajal, PROGRAM FullProf.2000 (Version 1.5) Multi-Pattern, Laboratoire Léon Brillouin (CEA-CNRS), France, April, 2000).
[10] G. Kresse, J. Furthmüller, Phys. Rev. B 54 (1996) 11169.
[11] G. Kresse, J. Furthmüller, Comput. Mater. Sci. 6 (1996) 15.
[12] P. Hohenberg, W. Kohn, Phys. Rev. 136 (1964) B864.
[13] W. Kohn, L.J. Sham, Phys. Rev. 140 (1965) A1133.
[14] J.P. Perdew, J.A. Chevary, S.H. Vosko, K.A. Jackson, M.R. Pederson, D.J. Singh, C. Fiolhais, Phys. Rev. B 46 (1992) 6671.
[15] P.E. Blöchl, Phys. Rev. B 50 (1994) 17953.
[16] G. Kresse, D. Joubert, Phys. Rev. B 59 (1999) 1758.
[17] H.J. Monkhorst, J.D. Pack, Phys. Rev. B 13 (1976) 5188.
[18] M. Methfessel, A.T. Paxton, Phys. Rev. B 40 (1989) 3616.
[19] D.S. Schreiber, R.M. Scotts, Phys. Rev. 131 (1963) 1118.
[20] G. Renaudin, P. Fischer, K. Yvon, J. Alloys Compd. 329 (2001) L9.